Received: 23 September 2024 | Accepted: 22 February 2025

DOI: 10.1002/jeo2.70219

ORIGINAL PAPER

Journal of Experimental Orthopaedics WILEY

Association of rotator cuff degeneration and scapular anatomy with humeral head migration in rotator cuff arthropathy

Hannes E. Tytgat[1] | **Nazanin Daneshvarhasjin**[1] | **Philippe Debeer**[1] | **Jean Chaoui**[2] | **Filip Verhaegen**[1]

[1]Department of Orthopedics, UZ Leuven, Leuven, Belgium

[2]Digital Technologies Trauma & Extremities, Stryker, Portage, Michigan, USA

Correspondence

Hannes E. Tytgat, Department of Orthopedics, Leuven, Herestraat 49, Sint-Kristoffelstraat 35, 2440 Geel, 3000 Leuven, Belgium.
Email: hannestytgat91@hotmail.com

Funding information

Zimmer-Biomet, Grant/Award Number: QPG-3C7801-VERHAEGEN-ZIMMER; Johson & Johnson, Grant/Award Number: EQQ-LSJJ04-O2010

Abstract

Purpose: Rotator cuff tear arthropathy (RCTA) is characterised by humeral head migration (HHM). The exact pathogenesis of HHM is poorly understood, although rotator cuff (RC) failure and scapular anatomy are thought to play an important role. The aim of this study is to investigate the possible association between HHM and the quantitative aspects of scapular anatomy and RC degeneration.

Methods: We analysed computed tomography scans of 43 RCTA patients. RC fatty infiltration (FI) and atrophy, HHM, and both native and pathologic scapular anatomy were quantitatively assessed in three dimensions.

Results: Patients with superior HHM had a significantly higher critical shoulder angle (34° vs. 30°, $p = 0.009$), and FI of the supraspinatus (26% vs. 16%, $p = 0.025$) and infraspinatus (IS) (25% vs. 16%, $p = 0.038$) compared to patients without superior HHM. Patients with posterior HHM had a significantly more retroverted native (mean 10° vs. 6°; $p = 0.002$) and pathologic glenoid (mean 11° vs. 4°; $p = 0.001$) and a higher anterior axis length (mean 40 mm vs. 37 mm; $p = 0.001$) compared to patients without anteroposterior HHM. Multivariate regression analysis showed that the native glenoid version, anterior axis length and the volume (Vol) of IS divided by subscapularis ($p = 0.01$) were independent predictors of the magnitude of anteroposterior HHM, together explaining 41% of its variance.

Conclusion: In RCTA, degeneration of the posterosuperior RC and acromion morphology seems to be associated with superior HHM, while in the glenoid version, the rotational alignment of the coracoacromial complex and an imbalance in FI and muscle Vol in the transverse force couple seems to be associated with anteroposterior HHM.

Level of Evidence: Level III.

KEYWORDS

glenoid version, humeral head migration, rotator cuff arthropathy, rotator cuff atrophy, rotator cuff fatty infiltration, scapular anatomy

Abbreviations: 2D, two-dimensional; CSA, critical shoulder angle; FI, fatty infiltration; FV, functional volume; HHM, humeral head migration; IS, infraspinatus; LAA, lateral acromial angle; PAS, posterior acromial slope; RC, rotator cuff; RCTA, rotator cuff tear arthropathy; SLD, subluxation distance; SLD-AP, SLD anteroposterior; SLD-SI, SLD superoinferior; SS, supraspinatus; Ssc, subscapularis; Vol, volume.

INTRODUCTION

Rotator cuff tear arthropathy (RCTA) is one of the most frequent types of shoulder arthropathy [23]. It represents a broad spectrum of pathology in which three critical factors are present: rotator cuff (RC) failure, humeral head migration (HHM) and glenohumeral joint degeneration [27]. The exact pathogenesis of RCTA remains unknown, but the hallmark is the failure of the RC. In the normal glenohumeral joint, the rotator cuff functions as a dynamic stabiliser by compressing the humeral head against the concave surface of the glenoid [19]. When those compressive forces fail to counteract the superior pull of the deltoid muscle, the humeral head can migrate superiorly, leading to the destruction of the humeral head and scapular bone [15, 18, 28]. While the superior HHM is most apparent and is incorporated in the definition of RCTA, there is also an important anteroposterior component to this HHM, but knowledge about its pathogenesis is limited [1, 6, 9]. A hypothesis is that posterior migration originates from the absence of the infraspinatus (IS) muscle combined with the posteriorly directed force of the latissimus dorsi, and similarly that anterior migration could occur due to the anterior pull of the pectoralis major in the absence of the subscapularis (Ssc) muscle [9, 13].

Previous research has investigated possible determinants of the quantitative aspects of HHM in RCTA, such as native scapular anatomy (e.g., native glenoid retroversion, acromion morphology and rotational alignment of the coracoacromial complex) [8, 9, 24], pathologic scapular anatomy [10, 14, 31] and RC degeneration [1, 15, 28]. RC degeneration can be characterised by fatty infiltration (FI) and muscle atrophy, which strongly correlate with muscle strength [17, 32]. Evidence of an association between HHM and RC degeneration is conflicting in shoulder OA [7, 29, 37], and even more limited in RCTA. In RCTA patients with posterosuperior glenoid erosion, FI was found to be much more pronounced in the posterosuperior RC compared to the Ssc [1]. Although an association between pathologic scapular anatomy and quantitative aspects of HHM can be intuitively expected, most studies could not find a correlation [10, 14, 36]. This lack of clear association of both pathologic scapular anatomy and RC degeneration with HHM is possibly due to methodological problems in the quantification of these parameters. Most studies used two-dimensional (2D) measurement techniques for quantification of HHM, RC degeneration and scapular anatomy, which has been shown to be less reliable [25, 31, 38]. In contrast, three-dimensional (3D) quantitative measurement techniques can improve the accuracy [3, 20, 31].

The aim of this study is to investigate the possible association between HHM on the one hand and the quantitative aspects of scapular anatomy and RC degeneration on the other hand. We hypothesise that (1) quantitative aspects of pathologic scapular anatomy and RC degeneration are associated with the amount of HHM, and more specifically (2), that the transverse force couple imbalance, together with glenoid version are associated with the amount of anteroposterior HHM.

MATERIALS AND METHODS

This retrospective case–control study was approved by the ethical committee of the University Hospitals Leuven (S58348). From a mixed computed tomography (CT) scan data set of patients undergoing reversed total shoulder arthroplasty and patients without radiographic signs of HHM or arthropathy (control group) as judged by an experienced shoulder surgeon (Filip Verhaegen), 64 patients with RCTA and 49 control patients were included based on the availability of the entire scapula and proximal humerus on the CT scan images, as previously reported in another study [9].

Quantification of rotator cuff degeneration

The soft-tissue Digital Imaging and Communications in Medicine (DICOM) images for each patient were uploaded into Mimics software (version 22.0; Materialise®). The scapular bone and the RC muscles supraspinatus (SS), Ssc and IS combined with teres minor were manually segmented by delineating the borders in the coronal, sagittal and axial plane [3, 38] (Figure 1a–e).

To quantify the RC muscle atrophy, the total muscle volume (Vol) of the different RC muscles was normalised to the patient's scapular bone Vol. To quantify the RC muscle FI, the fat Vol within each of the RC muscle Vols was determined based on a predefined threshold for fat (<−29 Hounsfield units [HU]) [30, 38] (Figure 1f). The obtained fat Vol was divided by the total muscle Vol, creating FI percentage within each cuff muscle. Finally, the functional volume (FV), representing the actual amount of RC muscle fibres, was calculated by subtracting the fat Volfrom from the total muscle Vol and then normalising it to the scapular bone Vol. The transverse force couple was defined as the obtained values for Vol, FI and FV of IS divided by Ssc [16], although Vol and FI are not the only determinants of force (e.g., fibre to muscle length ratio, fibre recruitment and angle of contraction).

Quantification of HHM

HHM was quantified with a previously reported and validated statistical shape model-based methodology [35]. In short, the native glenoid centre point and humeral head centre point, defined as the centre of mass of, respectively, all reconstructed glenoid surface

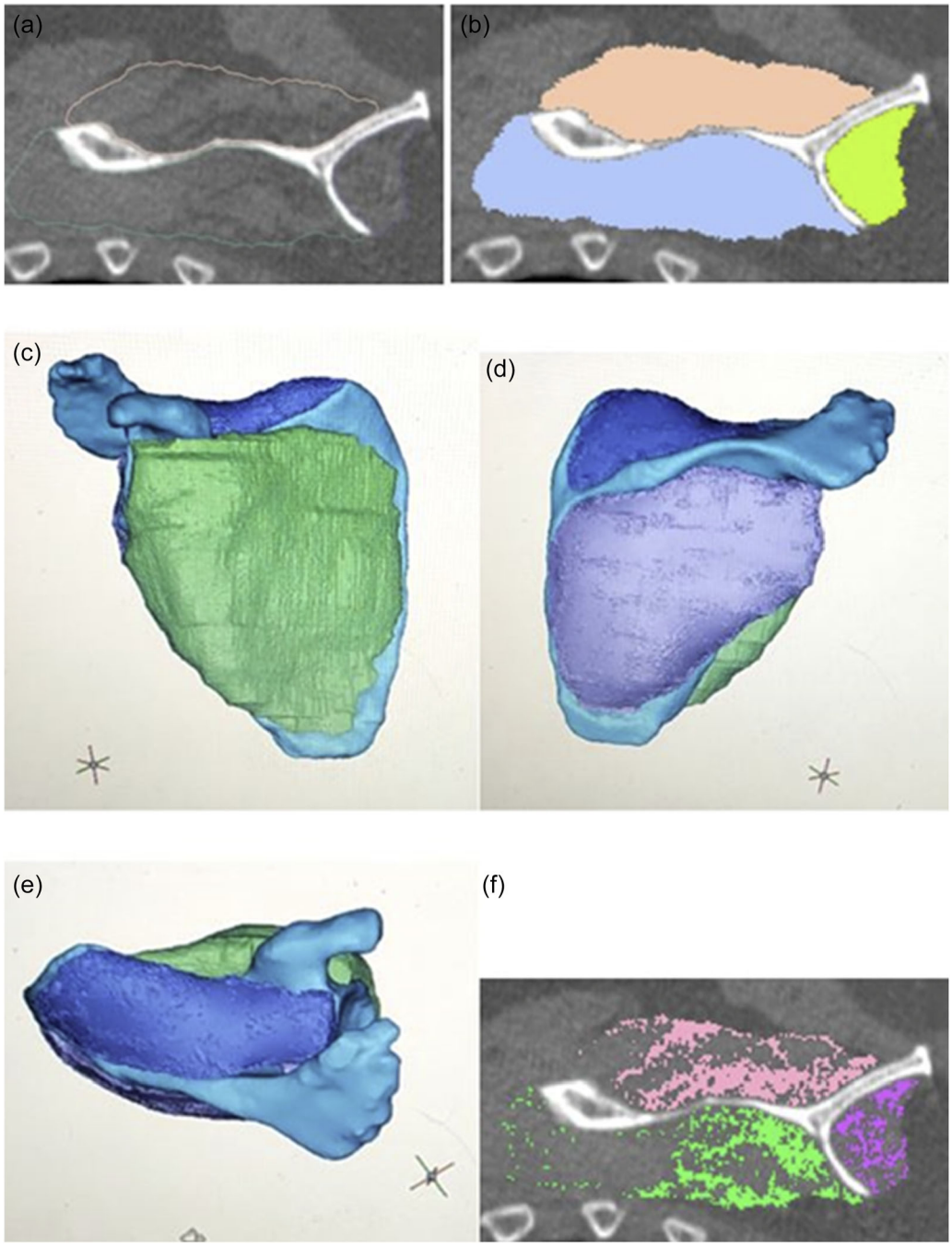

FIGURE 1 Quantification of rotator cuff degeneration. (a) Example of sagittal slice with delineated supraspinatus (blue), infraspinatus (orange) and subscapularis (green). (b) Example of sagittal slice depicting total muscle volume. (c–e) Example of 3D total muscle volume of RC muscles. (f) Sagittal slice depicting fatty tissue (<−29 HU) within each RC muscle. 3D, three-dimensional; HU, Hounsfield units; RC, rotator cuff.

points and all points of the proximal humerus are determined. The subluxation distance (SLD) is defined as the distance between the glenoid centre point and the projection of the humeral head centre point on the reconstructed glenoid plane. In addition, SLD is further divided into an anteroposterior (SLD-AP) and a superoinferior (SLD-SI) component based on the superior glenoid axis, which is the projection of the superior scapular axis on the reconstructed glenoid plane [9, 34]. A cut-off value for confirming HHM was based on the 'mean + 2 × standard deviation' of SLD in the control group. RCTA patients were grouped as 'RCTA with HHM (Group 1)' and 'RCTA without HHM (Group 2)'. Using the same methodology, a further subdivision was made in the anteroposterior and superoinferior direction, creating 'RCTA with posterior migration (Group 3)', 'RCTA with anterior migration (Group 4)', 'RCTA without anteroposterior migration (Group 5)', 'RCTA with superior

migration (Group 6)' and 'RCTA without superior migration (Group 7)'. The mean values and standard deviation of the control group and their resulting cut-off values can be found in Appendix S1.

Quantification of scapular anatomy

The parameters of the native scapular anatomy were automatically quantified with a previously published and validated 3D Statistical shape model-based methodology: native glenoid version and inclination, scapular offset, critical shoulder angle (CSA), lateral acromial angle (LAA), posterior acromial slope (PAS) and parameters describing the rotational alignment of the coracoacromial complex [22]. The pathologic scapular anatomy in terms of glenoid version and inclination was automatically quantified using the commercially available Glenosys software (Imascap®) [4].

Statistics

A priori power analysis was not performed due to the primarily explorative nature of this study. Descriptive statistics of RC degeneration, HHM, and scapular anatomy were performed for all groups. Normality of the variables was assessed by visual inspection of *Q*–*Q* plots and normality tests (Kolmogorov–Smirnov and Shapiro–Wilk). Statistical significance was considered at $p < 0.05$. Because of the non-normality of some parameters, the scapular anatomy and RC degeneration of Group 1 versus Group 2, and Group 6 versus Group 7 were evaluated with the Mann–Whitney *U* test, while the Kruskall–Wallis test was used for comparison between Groups 3 and 5. When the results were significant, pairwise (post hoc) comparisons were performed using the Mann–Whitney *U* test. To correct for Type I errors, a Bonferroni correction was applied, setting the significance level at $p < 0.02$. A stepwise multivariate regression analysis was performed to analyse the influence of the variables on the magnitude of SLD, SLD-AP and SLD-SI. In order to prevent overfitting of the models, we only included the parameters of the native scapular anatomy that were previously found to be significant determinants of HHM (LAA and CSA for SLD; native version and LAA for SLD-AP; scapular offset for SLD-SI) [9], and the other variables that were found to be significantly correlated after a univariate linear regression analysis ($p < 0.05$; $r < 0.33$ = weak; $0.33 < r > 0.66$ = moderate; $r > 0.66$ = strong).

RESULTS

Of the initial data set, 21 patients were excluded due to the absence of soft tissue windows on the available CT scan images, leaving a total of 43 patients for the RCTA group. Of this group, three patients were excluded from the pathologic scapular anatomy quantification because of the incompatibility of the CT scan images with the Glenosys software (Imascap®).

Rotator cuff degeneration

FI was more pronounced in the SS (mean 24%) and IS (mean 23%) compared to the Ssc (mean 10%, $p < 0.001$). The FV(Ssc) was the highest (1.15, $p < 0.001$). With regard to the transverse force couple, IS had a lower Vol and more FI than Ssc (mean Vol(IS/Ssc) 0.81; mean FI(IS/Ssc) 2.15) (Table 1).

Quantification of HHM and scapular anatomy

The mean SLD of the RCTA patients was 71% (SD ± 8%), and the mean SLD-AP and SLD-SI was 51% (SD ± 8%) and 69% (SD ± 9%), respectively. The mean SLD in Group 1 ($n = 34$) was 74% (SD 7%), as compared to 61% (SD3%) in Group 2 ($n = 9$, $p = 0.001$) (Figure 2a). As for anteroposterior HHM, Group 3 ($n = 15$) had a significantly higher SLD-AP of 60% (SD ± 5%, $p = 0.001$), compared to Group 4 ($n = 2$; SLD-AP = 35% ± SD 7%) and Group 5 ($n = 26$; SLD-AP = 47% ± SD 4%) (Figure 2b). Finally, Group 6 ($n = 33$) and Group 7 ($n = 10$) had a mean SLD-SI of 73 ± 6% and 58 ± 5% ($p = 0.001$) (Figure 2c), respectively.

The parameters of the native and pathologic scapula are shown in Table 2. The pathologic glenoid had a

TABLE 1 Quantification of rotator cuff degeneration in terms of volume (Vol), fatty infiltration (FI) and functional volume (FV).

		Mean (±SD)	*p* value
Vol	SS	0.36 (±0.06)	<0.001
	IS	1.09 (±0.17)	<0.001
	Ssc	1.32 (±0.24)	<0.001
	IS/Ssc[a]	0.81 (±0.15)	
FI	SS	0.24 (±0.12)	<0.001*
	IS	0.23 (±0.13)	<0.001*
	Ssc[a]	0.10 (±0.12)	<0.001
	IS/Ssc[a]	2.15 (±25.64)	
FV	SS	0.27 (±0.07)	<0.001
	IS	0.83 (±0.17)	<0.001
	Ssc	1.15 (±0.24)	<0.001
	IS/Ssc	0.76 (±0.22)	

Abbreviations: IS, infraspinatus; SS, supraspinatus; Ssc, subscapularis.
[a]Abnormally distributed with median value instead of mean.
*p value between FI(SS) and FI(IS) is 0.504.

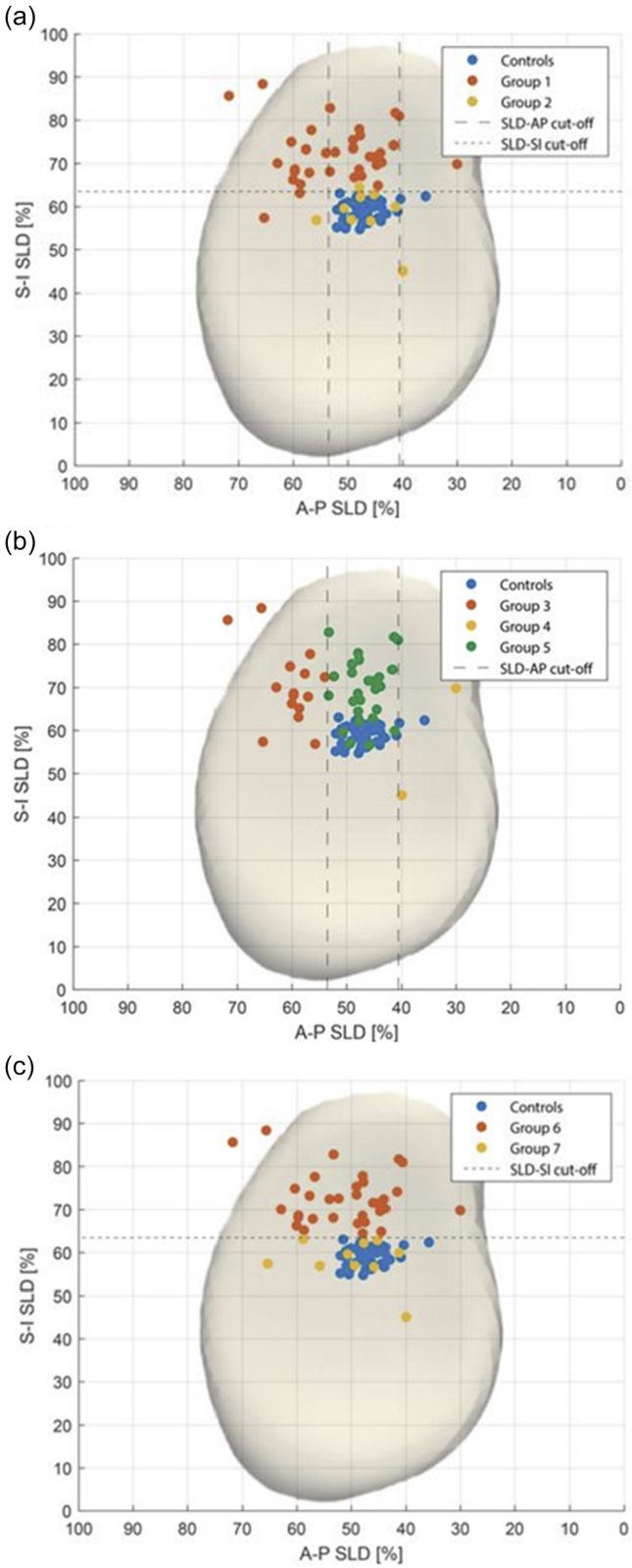

FIGURE 2 Polar plots from different subgroups. (a) Polar plot from control group, Group 1 (RCTA with HHM) and Group 2 (RCTA without HHM). (b) Polar plot from control group, Group 3 (RCTA with posterior HHM), Group 4 (RCTA with anterior HHM) and Group 5 (RCTA without AP HHM). (c) Polar plot from control group, Group 6 (RCTA with superior HHM) and Group 7 (RCTA without superior HHM). AP, anteroposterior; HHM, humeral head migration; RCTA, rotator cuff tear arthropathy.

mean retroversion of 7° (SD ± 7°) and a mean superior inclination of 12° (SD ± 6°).

Association of HHM with RC degeneration and scapular anatomy

Statistical analysis showed a significantly higher CSA (33° vs. 31°, $p = 0.039$) and LAA (95° vs. 91°, $p = 0.034$) for Group 1 in comparison to Group 2. In addition, the SS showed significantly more FI (26% vs. 16%, $p = 0.029$) for Group 1 (Table 3). The other parameters did not differ significantly between Groups 1 and 2. Univariate regression analysis showed a moderate correlation of SLD with FI(SS) ($r = 0.40$; $p = 0.008$), FI(IS) ($r = 0.39$; $p = 0.015$) and FV(IS) ($r = -0.34$; $p = 0.025$). Multiple regression analysis (including CSA, LAA, FI(SS), FI(IS) and FV(IS)) showed that FI(SS) was an independent significant predictor on the magnitude of SLD ($p = 0.008$) (see Appendix S2). Variance of SLD can be explained by FI(SS) for 14%. Regression predicts every increase of FI(SS) with 10% to be associated with an increase of SLD of 2.6% (95% confidence interval [CI]: 0.7–4.4).

Association of anteroposterior HHM with RC degeneration and scapular anatomy

Group 3 patients showed a significantly more retroverted native (mean 10° vs. 6°; $p = 0.002$) and pathologic glenoid (mean 11° vs. 4°; $p = 0.001$) and a higher anterior axis length (mean 40 mm vs. 37 mm; $p = 0.001$) compared to Group 5 (Table 4). Furthermore, there was a trend towards a smaller fulcrum axis ratio (44% vs. 47%, $p = 0.077$) and a higher Vol(IS/Ssc) (0.87 vs. 0.78; $p = 0.17$) in Group 3. No statistical significance was found between Group 4 and Group 3 or 5. Univariate regression analysis showed a moderate correlation of SLD-AP with anterior axis length ($r = 0.51$; $p < 0.001$), pathologic version ($r = 0.45$; $p = 0.004$) and Vol(IS/Ssc) ($r = 0.33$; $p = 0.03$), and a weak correlation with fulcrum axis ratio ($r = -0.31$; $p = 0.044$).

Multivariate regression analysis (including native and pathologic version, LAA, anterior axis length, Vol (IS/Ssc) and fulcrum axis ratio) showed that native version ($p = 0.002$), native version combined with Vol (IS/Ssc) ($p = 0.015$), and native version combined with Vol(IS/Ssc) and anterior axis length ($p = 0.01$) were independent significant predictors on the magnitude of SLD-AP (see Appendix S2). Variance of SLD-AP can be explained by these models as 21%, 31% and 41%, respectively. For the latter combination (native version combined with Vol(IS/Ssc) and anterior axis length), regression predicts every degree increase of native retroversion and every 1 mm increase of anterior axis length to be associated with an increase of

TABLE 2 Parameters of the native and pathologic scapula of all RCTA patients (mean ± SD).

	Mean (±SD)
Native inclination	8° (±4°)
Native version	7° (±4°)
Critical shoulder angle[a]	33° (±4°)
Posterior acromial slope	64° (±8°)
Lateral acromial angle	94° (±5°)
Scapular offset	102 mm (±6 mm)
Coracoid-scapula angle[a]	63° (±6°)
Anterior acromion-scapular plane angle	−1° (±9°)
Posterior acromion-scapular plane angle	56° (±8°)
Total fulcrum axis length	70 mm (±5 mm)
Fulcrum axis ratio[a]	45% (±4%)
Anterior axis length[a]	38 mm (±3 mm)
Posterior axis length	32 mm (±4 mm)
Glenoid translation	7 mm (± 3 mm)
Pathologic inclination	12° (±6°)
Pathologic version	7° (±7°)

Abbreviations: RCTA, rotator cuff tear arthropathy; SD, standard deviation.
[a]Abnormally distributed with median value instead of mean.

SLD-AP of 1% (95% CI: 0.07%–1.05% and 95% CI: 0.21%–1.43%, respectively). Every increase of Vol(IS/Ssc) with 0.1 is associated with an increase of SLD-AP of 2% (95% CI: 0.69%–3.35%).

Association of superoinferior HHM with RC degeneration and scapular anatomy

Group 6 had a significantly higher CSA (34° vs. 30°, $p = 0.009$), FI(SS) (26% vs. 16%, $p = 0.025$) and FI(IS) (25% vs. 16%, $p = 0.038$) compared to Group 7 (Table 5). There was also a trend towards a higher pathologic inclination (12° vs. 8°; $p = 0.139$). Univariate regression analysis showed a moderate correlation of SLD-SI with pathologic inclination ($r = 0.34$; $p = 0.03$), FI(SS) ($r = 0.42$; $p = 0.005$), FI(IS) ($r = 0.34$; $p = 0.024$) and FV(SS) ($r = -0.33$; $p = 0.032$), and a weak correlation with FV(IS) ($r = -0.31$; $p = 0.045$)

Multivariate regression analysis of SLD-SI (including scapular offset, pathologic inclination, FI(SS), FI(IS), FV(SS) and FV(IS)) showed that FV(IS) was an independent significant predictor on the magnitude of SLD-SI, explaining variance for 17% (see Appendix S2). Regression predicts every decrease of FV(IS) with 0.1 to be associated with an increase of SLD-SI of 2.5% (95% CI: −4.2 to −0.8).

DISCUSSION

The most important findings of this study are that degeneration of the posterosuperior RC, pathologic superior glenoid inclination and acromion morphology are associated with superior HHM, while glenoid version, transverse force couple imbalance and the rotational alignment of the coracoacromial complex are associated with anteroposterior HHM.

We found a moderate correlation between FI and FV of the posterosuperior RC and superior HHM. This is in accordance with previous findings, which showed that superior HHM occurs when an RC tear extends from the SS to the IS [15, 18, 28]. We also found that RCTA patients with superior HHM had a significantly higher CSA. A high CSA, which is influenced by the lateral extension of the acromion and the glenoid inclination, has been previously reported to be associated with increased risk and magnitude of RC failure, as well as increased superior HHM [8, 24]. The postulated patho-mechanism is believed to be twofold, with, on the one hand, an increased compression of the SS tendon and, on the other hand, an increased ascending force vector and decreased compressive force vector of the middle deltoid [24]. When controlling for confounding variables in a multivariate regression analysis, only FV(IS) remained as an independent significant predictor. Interestingly, scapular anatomy was not withheld as an independent predictor. This could suggest that superior HHM is mostly soft tissue driven.

Regarding the anteroposterior direction of HHM, our results show a significantly higher native and pathologic glenoid retroversion in case of posterior HHM. This is in accordance with previous research on shoulder OA, which showed a significantly higher native retroversion in patients with posterior HHM [9, 33] and a high correlation between HHM and pathologic glenoid version, both in amplitude and direction [31]. Secondly, we found that the anterior axis length was significantly larger in patients with posterior HHM. It is the distance between the coracoid and the intersection of the scapular plane with the fulcrum axis, which runs from the posterior acromion to the coracoid [22]. This indicates a more anteriorly translated coracoacromial arch relative to the scapular plane. These findings are in line with those in shoulder OA [33]. Finally, the influence of the RC on anteroposterior HHM in RCTA is not yet fully understood. The muscle Vol and FI of the transverse force couple are in equilibrium in non-pathologic shoulders [16, 26]. The current hypothesis is that posterior HHM originates from the absence of the IS muscle combined with the posteriorly directed force of the latissimus dorsi [13]. Although we found a less voluminous posterior RC in all groups and subgroups of RCTA patients (Vol(IS/Ssc) < 1), there was a trend towards a higher Vol(IS/Ssc) in posterior

TABLE 3 Parameters of RC degeneration and scapular anatomy for Groups 1 and 2 (mean ± SD).

	Group 1: with HHM ($n = 34$)	Group 2: without HHM ($n = 9$)	p value
Native inclination	8° (±4°)	6° (±5°)	0.199
Native version	8° (±5°)	6° (±3°)	0.339
Critical shoulder angle[a]	**33° (±4°)**	**31° (±3°)**	**0.039**
Posterior acromial slope	64° (±9°)	65° (±7°)	0.881
Lateral acromial angle	**95° (±5°)**	**91° (±5°)**	**0.034**
Scapular offset	103 mm (±6 mm)	102 mm (±6 mm)	0.676
Coracoid-scapula angle[a]	64° (±5°)	60° (±7°)	0.31
Anterior acromion-scapular plane angle	−1° (±9°)	0° (±9°)	0.591
Posterior acromion-scapular plane angle	56° (±8°)	56° (±8°)	0.788
Total fulcrum axis length	70 mm (±6 mm)	71 mm (±4 mm)	0.244
Fulcrum axis ratio[a]	46% (±4%)	45% (±5%)	0.55
Anterior axis length[a]	38 mm (±3 mm)	37 mm (±4 mm)	0.834
Posterior axis length	32 mm (±5 mm)	33 mm (±4 mm)	0.42
Glenoid translation	6 mm (±6 mm)	7 mm (±2 mm)	0.455
Pathologic inclination	12° (±6°)	9° (±6°)	0.144
Pathologic version	7° (±7°)	6° (±5°)	0.773
Vol(SS)	0.36 (±0.07)	0.35 (±0.05)	0.976
FI(SS)	**0.26 (±0.13)**	**0.16 (±0.08)**	**0.029**
Vol(IS)	1.09 (±0.17)	1.08 (±0.19)	0.698
FI(IS)	0.24 (±0.14)	0.19 (±0.12)	0.325
Vol(Ssc)	1.31 (±0.26)	1.38 (±0.17)	0.339
FI(Ssc)[a]	0.10 (±0.13)	0.07 (±0.06)	0.199
Vol(IS/Ssc)[a]	0.81 (±0.15)	0.78 (±0.11)	0.355
FI(IS/Ssc)[a]	1.83 (±28.83)	2.67 (±1.97)	0.403
FV(SS)	0.27 (±0.07)	0.30 (±0.06)	0.152
FV(IS)	0.82 (±0.15)	0.89 (±0.24)	0.21
FV(Ssc)	1.11 (±0.25)	1.27 (±0.20)	0.064
FV(IS/Ssc)	0.77 (±0.23)	0.70 (±0.16)	0.571

Note: Underline bold values are statistical significant results.

Abbreviations: FI, fatty infiltration; FV, functional volume; IS, infraspinatus; SS, supraspinatus; Ssc, subscapularis; Vol, volume.

[a]Abnormally distributed with median value instead of mean.

HHM and an increase of Vol(IS/Ssc) was associated with an increase of posterior HHM. These findings seem to contradict the current hypothesis. To our knowledge, only one study investigated the influence of RC degeneration in RCTA on glenoid erosion [1], which correlates strongly with HHM when assessed in 3D [31]. They found that FI was more pronounced in the posterosuperior RC in RCTA patients with posterosuperior glenoid erosion. Contrastingly, an increase in Ssc FI was associated with an increase in posterior glenoid erosion. In shoulder OA, Aleem et al. found a higher IS/Ssc Vol in case of posterior HHM, which is in line with our findings [2]. Others found conflicting results [7, 29, 30, 37]. However, the aforementioned studies used 2D measurement techniques, which are less reliable [20, 30, 31]. Using a similar 3D technique as ours, Arenas-Miquelez et al. found no difference in the IS/Ssc Vol between shoulder OA patients with and without posterior HHM [3]. They did find a higher FI ratio of IS/Ssc to be significantly associated with posterior HHM. They postulated that this was likely to be a consequence of posterior HHM, as posterior HHM

TABLE 4 Parameters of RC degeneration and scapular anatomy for Groups 3, 4 and 5 (mean ± SD).

	Group 3: anterior HHM ($n = 15$)	Group 4: posterior HHM ($n = 2$)	Group 5: no AP HHM ($n = 26$)	p value	Group 3 vs. Group 5
Native inclination	9° (±4°)	6° (±4°)	7° (±4°)	0.382	
Native version	**10° (±4°)**	**7° (±4°)**	**6° (±4°)**	**0.008**	**0.002**
Critical shoulder angle[a]	32° (±5°)	31° (±8°)	33° (±4°)	0.92	
Posterior acromial slope	65° (±9°)	60° (±1°)	64° (±8°)	0.725	
Lateral acromial angle	94° (±5°)	92° (±5°)	94° (±6°)	0.738	
Scapular offset	104 mm (±5 mm)	98 mm (±1 mm)	102 mm (±6 mm)	0.332	
Coracoid-scapula angle[a]	65° (±5°)	57° (±6°)	61° (±5°)	0.11	
Anterior acromion-scapular plane angle	0° (±9°)	−8° (±3°)	−1° (±10°)	0.486	
Posterior acromion-scapular plane angle	54° (±10°)	57° (±5°)	57° (±6°)	0.654	
Total fulcrum axis length	72 mm (±6 mm)	68 mm (±3 mm)	69 mm (±5 mm)	0.153	
Fulcrum axis ratio[a]	44% (±5%)	48% (±1%)	47% (±3%)	0.077	
Anterior axis length[a]	**40 mm (±4 mm)**	**35 mm (±1 mm)**	**37 mm (±2 mm)**	**0.001**	**0.001**
Posterior axis length	32 mm (±5 mm)	33 mm (±2 mm)	32 mm (±4 mm)	0.599	
Glenoid translation	6 mm (±3 mm)	6 mm (±mm)	7 mm (±3 mm)	0.354	
Pathologic inclination	12° (±6°)	−1°	12° (±5°)	0.237	
Pathologic version	**11° (±6°)**	**7°**	**4° (±6°)**	**0.003**	**0.001**
Vol(SS)	0.37 (±0.06)	0.35 (±0.06)	0.35 (±0.07)	0.429	
FI(SS)	0.26 (±0.10)	0.23 (±0.26)	0.22 (±0.13)	0.346	
Vol(IS)	1.14 (±0.15)	1.13 (±0.12)	1.05 (±0.13)	0.317	
FI(IS)	0.24 (±0.11)	0.31 (±0.32)	0.22 (±0.13)	0.725	
Vol(Ssc)	1.30 (±0.25)	1.34 (±0.16)	1.33 (±0.24)	0.945	
FI(Ssc)[a]	0.10 (±0.12)	0.26 (±0.11)	0.08 (±0.12)	0.183	
Vol(IS/Ssc)[a]	0.87 (±0.17)	0.85 (±0.19)	0.78 (±0.13)	0.17	
FI(IS/Ssc)[a]	2.01 (±43.29)	1.02 (±0.79)	2.23 (±1.92)	0.4	
FV(SS)	0.28 (±0.06)	0.28 (±0.14)	0.27 (±0.06)	0.993	
FV(IS)	0.86 (±0.13)	0.76 (±0.28)	0.82 (±0.18)	0.768	
FV(Ssc)	1.13 (±0.27)	1.00 (±0.27)	1.17 (±0.23)	0.484	
FV(IS/Ssc)	0.82 (±0.28)	0.75 (±0.08)	0.72 (±0.19)	0.649	

Abbreviations: FI, fatty infiltration; FV, functional volume; IS, infraspinatus; RC, rotator cuff; SS, supraspinatus; Ssc, subscapularis; Vol, volume.
[a]Abnormally distributed with median value instead of mean.

causes a disturbed length–tension relationship with an increase in pennation angle and reduction of sarcomeres, which is shown to cause FI [11, 12, 21]. These contradictory findings seem to indicate that we have yet to discover the exact relationship between AP-HHM and transverse force couple imbalance. It is clear, however, that bony scapular anatomy plays an important role in posterior HHM, as it can explain 31% of AP-HHM variance.

The strength of the study is the use of highly accurate, state-of-the-art 3D quantitative assessment of RC degeneration, scapular anatomy and HHM. 2D assessment of RC degeneration is most frequently used in other studies but is less accurate because the distribution of intra-muscular fat is not uniform in the RC muscles [38] and because the cross-sectional area of the RC muscle can be influenced by HHM [3]. Also, most previous studies used the Goutallier classification

TABLE 5 Parameters of RC degeneration and scapular anatomy for Groups 6 and 7 (mean ± SD).

	Group 6: superior HHM ($n = 33$) Mean	Group 7: no superior HHM ($n = 10$) Mean	p value
Native inclination	8° (±4°)	6° (±5°)	0.262
Native version	7° (±4°)	8° (±5°)	0.646
Critical shoulder angle[a]	**34° (±4°)**	**30° (±3°)**	**0.009**
Posterior acromial slope	64° (±9°)	65° (±6°)	0.931
Lateral acromial angle	95° (±6°)	92° (±5°)	0.135
Scapular offset	103 mm (±6 mm)	102 mm (±6 mm)	0.687
Coracoid-scapula angle[a]	64° (±5°)	61° (±8°)	0.666
Anterior acromion-scapular plane angle	−1° (±10°)	−1° (±9°)	0.73
Posterior acromion-scapular plane angle	56° (±8°)	56° (±8°)	0.646
Total fulcrum axis length	70 mm (±6 mm)	71 mm (±4 mm)	0.287
Fulcrum axis ratio[a]	46% (±4%)	45% (±5%)	0.908
Anterior axis length[a]	38 mm (±3 mm)	37 mm (±4 mm)	0.709
Posterior axis length	32 mm (±5 mm)	32 mm (±4 mm)	0.752
Glenoid translation	7 mm (±3 mm)	6 mm (±3 mm)	0.908
pathologic inclination	12° (±6°)	8° (±7°)	0.139
pathologic version	6° (±7°)	9° (±5°)	0.243
Vol(SS)	0.36 (±0.07)	0.35 (±0.06)	1
FI(SS)	**0.26 (±0.12)**	**0.16 (±0.10)**	**0.025**
Vol(IS)	1.10 (±0.17)	1.05 (±0.18)	0.687
FI(IS)	**0,25 (±0.14)**	**0,16 (±0.10)**	**0.038**
Vol(Ssc)	1.34 (±0.25)	1.28 (±0.22)	0.585
FI(Ssc)[a]	0.10 (±0.13)	0.06 (±0.08)	0.301
Vol(IS/Ssc)[a]	0.81 (±0.14)	0.82 (±0.17)	1
FI(IS/Ssc)[a]	2.01 (±29.25)	2.48 (±1.96)	0.863
FV(SS)	0.26 (±0.06)	0.30 (±0.07)	0.216
FV(IS)	0.81 (±0.15)	0.90 (±0.23)	0.121
FV(Ssc)	1.14 (±0.24)	1.17 (±0.25)	0.565
FV(IS/Ssc)	0.74 (±0.21)	0.79 (±0.26)	0.546

Abbreviations: FI, fatty infiltration; FV, functional volume; IS, infraspinatus; SS, supraspinatus; Ssc, subscapularis; Vol, volume.
[a]Abnormally distributed with median value instead of mean.

for assessing FI, which is limited due to its poor inter-observer and intra-observer reliability and its qualitative characteristics [20, 25]. Second, to our knowledge, this is the first study to incorporate RC degeneration, and native and pathologic scapular anatomy to investigate their association with HHM.

Nevertheless, this study has several limitations as well. First of all, we did not assess RC integrity. We opted to use FI and Vol of the RC muscles to account for their function, as they are shown to be directly related to force generation capacity [17, 26, 32]. Furthermore, FI and atrophy are shown to occur as a result of tendon injury [11, 12, 21]. Second, patient age and sex were not included in the analysis. Although FI is not influenced by age or sex in healthy shoulders, there is a significant difference in muscle Vol between males and females [16]. This may have caused less reliable results regarding the influence of RC atrophy on HHM. Thirdly, our data set was rather small, making our statistical analysis possibly underpowered to detect other significant associations. Finally, our models for explaining the variance of anteroposterior and superior

HHM only reached 41% and 17%, respectively. Therefore, further research is mandatory and should include dynamic RC activation, other shoulder muscles (such as deltoid, latissimus dorsi and pectoralis major) [5] and scapulothoracic motion and position.

CONCLUSION

In RCTA, degeneration of the posterosuperior RC and acromion morphology seems to be associated with superior HHM, while in the glenoid version, the rotational alignment of the coracoacromial complex and an imbalance in FI and muscle Vol in the transverse force couple seems to be associated with anteroposterior HHM.

AUTHOR CONTRIBUTIONS

Hannes E. Tytgat: Analysis and interpretation of data/drafting the paper. **Nazanin Daneshvarhasjin**: Acquisition of data. **Philippe Debeer**: Approval of the final version. **Jean Chaoui**: Acquisition of data. **Filip Verhaegen**: Research design/critical revision of paper.

ACKNOWLEDGEMENTS

The Institute for Orthopaedic Research and Training (IORT), Department of Development and Regeneration, KU Leuven, Division of Orthopaedics, University Hospitals Leuven reports research grant funding from the following organisations broadly related to the topic of this work: Zimmer-Biomet (QPG-3C7801-VERHAEGEN-ZIMMER GMBH) and Johson & Johnson (EQQ-LSJJ04-O2010). None of these outside sources or funders were involved in the study design, data collection, data analysis, or the preparation or editing of the manuscript. The IORT, Philippe Debeer and Filip Verhaegen report consultancy agreements with Materialise N.V. (Leuven, Belgium) and Exactech INC (2320 NW 66th Court, Gainesville, Florida). These relationships have no bias on this work and did not inappropriately influence this study.

CONFLICT OF INTEREST STATEMENT

The authors declare no conflicts of interest.

DATA AVAILABILITY STATEMENT

The data that support the findings of this study are available from the corresponding author upon request.

ETHICS STATEMENT

This study was approved by the Ethics Committee Research UZ/KU Leuven (S58348). Informed consent was obtained from all individual participants included in the study.

ORCID

Hannes E. Tytgat http://orcid.org/0000-0003-1702-0107

REFERENCES

1. Abdic S, Knowles NK, Walch G, Johnson JA, Athwal GS. Type E2 glenoid bone loss orientation and management with augmented implants. J Shoulder Elbow Surg. 2020;29(7):1460–9.
2. Aleem AW, Chalmers PN, Bechtold D, Khan AZ, Tashjian RZ, Keener JD. Association between rotator cuff muscle size and glenoid deformity in primary glenohumeral osteoarthritis. J Bone Jt Surg. 2019;101:1912–20.
3. Arenas-Miquelez A, Liu VK, Cavanagh J, Graham PL, Ferreira LM, Bokor DJ, et al. Does the Walch type B shoulder have a transverse force couple imbalance? A volumetric analysis of segmented rotator cuff muscles in osteoarthritic shoulders. J Shoulder Elbow Surg. 2021;30(10):2344–54.
4. Boileau P, Cheval D, Gauci MO, Holzer N, Chaoui J, Walch G. Automated three-dimensional measurement of glenoid version and inclination in arthritic shoulders. J Bone Jt Surg. 2018;100(1):57–65.
5. Campbell ST, Ecklund KJ, Chu EH, McGarry MH, Gupta R, Lee TQ. The role of pectoralis major and latissimus dorsi muscles in a biomechanical model of massive rotator cuff tear. J Shoulder Elbow Surg. 2014;23(8):1136–42.
6. Collins DN, Harryman DT. Arthroplasty for arthritis and rotator cuff deficiency. Orthop Clin North Am. 1997;28(2):225–39.
7. Donohue KW, Ricchetti ET, Ho JC, Iannotti JP. The association between rotator cuff muscle fatty infiltration and glenoid morphology in glenohumeral osteoarthritis. J Bone Jt Surg. 2018;100(5):381–7.
8. Engelhardt C, Farron A, Becce F, Place N, Pioletti DP, Terrier A. Effects of glenoid inclination and acromion index on humeral head translation and glenoid articular cartilage strain. J Shoulder Elbow Surg. 2017;26(1):157–64.
9. Verhaegen F, Meynen A, Plessers K, Scheys L, Debeer P. Quantitative SSM-based analysis of humeral head migration in rotator cuff tear arthropathy patients. J Orthop Res. 2021;40:1707–14.
10. Gerber C, Costouros JG, Sukthankar A, Fucentese SF. Static posterior humeral head subluxation and total shoulder arthroplasty. J Shoulder Elbow Surg. 2009;18(4):505–10.
11. Gerber C, Meyer DC, Frey E, von Rechenberg B, Hoppeler H, Frigg R, et al. Neer Award 2007: reversion of structural muscle changes caused by chronic rotator cuff tears using continuous musculotendinous traction. An experimental study in sheep. J Shoulder Elbow Surg. 2009;18(2):163–71.
12. Gerber C, Meyer DC, Schneeberger AG, Hoppeler H, Von Rechenberg B. Effect of tendon release and delayed repair on the structure of the muscles of the rotator cuff: an experimental study in sheep. J Bone Joint Surg Am. 2004;86(9):1973–82.
13. Goutallier D, Le Guilloux P, Postel JM, Radier C, Bernageau J, Zilber S. Acromio humeral distance less than six millimeter: its meaning in full-thickness rotator cuff tear. Orthop Traumatol Surg Res. 2011;97(3):246–51.
14. Hoenecke HR, Tibor LM, D'Lima DD. Glenoid morphology rather than version predicts humeral subluxation: a different perspective on the glenoid in total shoulder arthroplasty. J Shoulder Elbow Surg. 2012;21(9):1136–41.
15. Itami Y, Park MC, Lin CC, Patel NA, McGarry MH, Park CJ, et al. Biomechanical analysis of progressive rotator cuff tendon tears on superior stability of the shoulder. J Shoulder Elbow Surg. 2021;30(11):2611–9.
16. Kälin PS, Crawford RJ, Marcon M, Manoliu A, Bouaicha S, Fischer MA, et al. Shoulder muscle volume and fat content in healthy adult volunteers: quantification with DIXON MRI to determine the influence of demographics and handedness. Skeletal Radiol. 2018;47(10):1393–402.
17. Karampinos DC, Holwein C, Buchmann S, Baum T, Ruschke S, Gersing AS, et al. Proton density fat-fraction of rotator cuff

muscles is associated with isometric strength 10 years after rotator cuff repair: a quantitative magnetic resonance imaging study of the shoulder. Am J Sports Med. 2017;45(9):1990–9.
18. Keener JD, Wei AS, Kim HM, Steger-May K, Yamaguchi K. Proximal humeral migration in shoulders with symptomatic and asymptomatic rotator cuff tears. J Bone Joint Surg Am. 2009;91(6):1405–13.
19. Labriola JE, Lee TQ, Debski RE, McMahon PJ. Stability and instability of the glenohumeral joint: the role of shoulder muscles. J Shoulder Elbow Surg. 2005;14(1 Suppl):32–8.
20. Lee E, Choi JA, Oh JH, Ahn S, Hong SH, Chai JW, et al. Fatty degeneration of the rotator cuff muscles on pre- and postoperative CT arthrography (CTA): is the Goutallier grading system reliable? Skeletal Radiol. 2013;42(9):1259–67.
21. Meyer DC, Hoppeler H, von Rechenberg B, Gerber C. A pathomechanical concept explains muscle loss and fatty muscular changes following surgical tendon release. J Orthop Res. 2004;22(5):1004–7.
22. Naidoo N, Lazarus L, Satyapal KS, De Wilde L, Van Tongel A. The morphometric anatomy of the delto-fulcral triangle: a 3D CT-based reconstruction study. J Orthop. 2017;14(1):62–7.
23. Neer CS, Craig EV, Fukuda H. Cuff-tear arthropathy. J Bone Joint Surg. 1983;65(9):1232–44.
24. Nyffeler RW, Meyer DC. Acromion and glenoid shape: why are they important predictive factors for the future of our shoulders. EFORT Open Rev. 2017;2(5):141–50.
25. Oh JH, Kim SH, Choi JA, Kim Y, Oh CH. Reliability of the grading system for fatty degeneration of rotator cuff muscles. Clin Orthop Relat Res. 2010;468(6):1558–64.
26. Piepers I, Boudt P, Van Tongel A, De Wilde L. Evaluation of the muscle volumes of the transverse rotator cuff force couple in nonpathologic shoulders. J Shoulder Elbow Surg. 2014;23(7):e158–62.
27. Rugg CM, Gallo RA, Craig EV, Feeley BT. The pathogenesis and management of cuff tear arthropathy. J Shoulder Elbow Surg. 2018;27(12):2271–83.
28. Sahara W, Yamazaki T, Inui T, Konda S. Three-dimensional kinematic features in large and massive rotator cuff tears with pseudoparesis. J Shoulder Elbow Surg. 2021;30(4):720–8.
29. Siebert MJ, Chalian M, Sharifi A, Pezeshk P, Xi Y, Lawson P, et al. Correction to: qualitative and quantitative analysis of glenoid bone stock and glenoid version: inter-reader analysis and correlation with rotator cuff tendinopathy and atrophy in patients with shoulder osteoarthritis. Skeletal Radiol. 2020;49(6):995–1003.
30. Terrier A, Ston J, Dewarrat A, Becce F, Farron A. A semi-automated quantitative CT method for measuring rotator cuff muscle degeneration in shoulders with primary osteoarthritis. Clin Orthop Relat Res. 2017;103(2):151–7.
31. Terrier A, Ston J, Farron A. Importance of a three-dimensional measure of humeral head subluxation in osteoarthritic shoulders. J Shoulder Elbow Surg. 2015;24(2):295–301.
32. Valencia AP, Lai JK, Iyer SR, Mistretta KL, Spangenburg EE, Davis DL, et al. Fatty infiltration is a prognostic marker of muscle function after rotator cuff tear. Am J Sports Med. 2018;46(9):2161–9.
33. Verhaegen F, Meynen A, Debeer P, Scheys L. Determination of predisposing scapular anatomy with a statistical shape model—part II: shoulder osteoarthritis. J Shoulder Elbow Surg. 2021;30(9):e558–71.
34. Verhaegen F, Meynen A, Pitocchi J, Debeer P, Scheys L. Quantitative statistical shape model-based analysis of humeral head migration, Part 2: shoulder osteoarthritis. J Orthop Res. 2023;41(1):21–31.
35. Verhaegen F, Meynen A, Plessers K, Scheys J, Debeer P. Quantitative SSM-based analysis of humeral head migration in rotator cuff tear arthropathy patients. J Orthop Res. 2021;40(7):7–14.
36. Walch G, Badet R, Boulahia A, Khoury A. Morphologic study of the glenoid in primary glenohumeral osteoarthritis. J Arthroplasty. 1999;14(6):756–60.
37. Walker KE, Simcock XC, Jun BJ, Iannotti JP, Ricchetti ET. Progression of glenoid morphology in glenohumeral osteoarthritis. J Bone Jt Surg Am. 2018;100(1):49–56.
38. Werthel J-D, Boux de Casson F, Walch G, Gaudin P, Moroder P, Sanchez-Sotelo J, et al. 3D Muscle Loss (3DML) assessment: a novel CT-based quantitative method to evaluate rotator cuff muscle fatty infiltration. J Shoulder Elbow Surg. 2022;31(1):165–74.

SUPPORTING INFORMATION

Additional supporting information can be found online in the Supporting Information section at the end of this article.

How to cite this article: Tytgat HE, Daneshvarhasjin N, Debeer P, Chaoui J, Verhaegen F. Association of rotator cuff degeneration and scapular anatomy with humeral head migration in rotator cuff arthropathy. J Exp Orthop. 2025;12:e70219. https://doi.org/10.1002/jeo2.70219